

Online Attentive Kernel-Based Temporal Difference Learning

Guang Yang, Xingguo Chen, Shangdong Yang, Huihui Wang, Shaokang Dong, Yang Gao

With rising uncertainty in the real world, online Reinforcement Learning (RL) has been receiving increasing attention due to its fast learning capability and improving data efficiency. However, online RL often suffers from complex Value Function Approximation (VFA) and catastrophic interference, creating difficulty for the deep neural network to be applied to an online RL algorithm in a fully online setting. Therefore, a simpler and more adaptive approach is introduced to evaluate value function with the kernel-based model. Sparse representations are superior at handling interference, indicating that competitive sparse representations should be learnable, non-prior, non-truncated and explicit when compared with current sparse representation methods. Moreover, in learning sparse representations, attention mechanisms are utilized to represent the degree of sparsification, and a smooth attentive function is introduced into the kernel-based VFA. In this paper, we propose an Online Attentive Kernel-Based Temporal Difference (OAKTD) algorithm using two-timescale optimization and provide convergence analysis of our proposed algorithm. Experimental evaluations showed that OAKTD outperformed several Online Kernel-based Temporal Difference (OKTD) learning algorithms in addition to the Temporal Difference (TD) learning algorithm with Tile Coding on public Mountain Car, Acrobot, CartPole and Puddle World tasks.

Index Terms—Online Reinforcement Learning, kernel-based value function, sparse representation, attentive function, two-timescale optimization.

I. INTRODUCTION

IN Reinforcement Learning (RL), an agent usually seeks the optimal policy and learns it to solve a sequential decision-making problem [1], and the entire learning process relies heavily on the interaction between agent and working environment. In practice, real-world problems are complex and indefinite, often resulting in ineffective and inefficient computation and learning during long episodic applications while using offline algorithms. To solve these problems, online RL has been proposed, a solution gaining recent widespread attention [2], especially online RL methods for fully online updating which rely on one transition[3], which is current and limited transition or experience, e.g., Temporal Difference (TD) learning [4]. Online RL can result in faster learning

through bootstrapping and improved computational and data efficiency because it focuses on learning from real-time samples which are encountered frequently. However, online RL implementation still needs to consider the following issues:

- Online RL requires a function approximation that can work effectively in online learning rather than offline or batch learning.
- Online updating often suffers from catastrophic forgetting or interference.
- Online algorithms should possess good convergence guarantees.

Value Function Approximation (VFA) is a widely used RL technique for large-scale or continuous state spaces. In general, it is a mapping of features and related parameters to state values, which can be divided into linear and nonlinear methods. As a representative of nonlinear VFA, learning from batch updating and deep neural networks [5] often fails to solve simple RL tasks in fully online settings [2]. Compared with deep neural networks, linear VFA methods can be computed quickly and exhibit elegant theoretical analysis [6], [7], [8], however, their performance often depends on features defined by experts. Fortunately, kernel-based VFA is an ideal choice for online RL, as it can not only learn representations adaptively [9], but also learn in fully online settings [10].

When online RL uses VFA, an update on one transition may change all parameters of the value function. This issue, referred to catastrophic interference, causes the update on the current transition to catastrophically interfere with or forget the updates on previous transitions. Generally, an effective method for resolving catastrophic interference in online RL is sparse representation [2], where only partial parameters need updating to reduce global interference. In addition, sparse representation can capture important state attributes so that the agent can obtain an accurate value evaluation.

Traditional sparse representation methods such as Tile Coding [11] and n-tuple networks [12], have been successfully applied in linear VFA algorithms, but they are artificially predefined and limited by the curse of dimensionality. For neural networks, there are certain methods that can be used for sparse representation: (i) Rectified Linear Units (ReLU) [13] is learnable and imply sparsity, but provides no such guarantees. To further promote sparsity, some heuristics have been proposed to reduce catastrophic interference. (ii) Dropout randomly masks part of the activation function during training [14]. (iii) k -sparse autoencoders only retain the top- k nodes largest activations [15]. (iv) Winner-Take-All autoencoders keep the first $k\%$ activations of each layer in the training [16]. Although they suited for high-dimensional inputs, they are problematic, as they have a tendency truncate potentially

G. Yang and X. Chen are with the the Jiangsu Key Laboratory of Big Data Security & Intelligent Processing, Nanjing University of Posts and Telecommunications, and National Engineering Laboratory for Agri-product Quality Traceability, Beijing Technology and Business University, P.R., China (e-mail: guangyang9543@gmail.com; chenxg@njupt.edu.cn). (Corresponding author: X. Chen.)

S. Yang, S. Dong and Y. Gao are with the State Key Laboratory for Novel Software Technology, Nanjing University, P.R., China (e-mail: shaokangdong@gmail.com, yangshangdong007@gmail.com, gaoy@nju.edu.cn)

H. Wang is with the PCA Lab, Key Lab of Intelligent Perception and Systems for High-Dimensional Information of Ministry of Education, and Jiangsu Key Lab of Image and Video Understanding for Social Security, School of Computer Science and Engineering, Nanjing University of Science and Technology, P. R., China (e-mail: Huihuiwang@njjust.edu.cn).

TABLE I

COMPARISON OF VARIOUS SPARSE REPRESENTATIONS ON FOUR ASPECTS: “Learnable” refers to the ability to adaptively learn a sparse representation without artificial construction; “Non-prior” means that no prior knowledge or hyperparameters are required; “Non-truncated” signifies a continuous or smooth reduction (not discretization); “Explicit” means that the value function is represented by an explicit sparse mechanism.

| Sparse Representations | Learnable | Non-prior | Non-truncated | Explicit |
|-----------------------------------|-----------|-----------|---------------|----------|
| Tile Coding [11] | | | | ✓ |
| n-tuple networks [12] | | | | ✓ |
| ReLU [13] | ✓ | ✓ | | |
| Dropout [14] | | | | ✓ |
| k -sparse autoencoders [15] | | | | ✓ |
| Winner-Take-All autoencoders [16] | | | | ✓ |
| L_1 regularization [17] | ✓ | | | ✓ |
| L_2 regularization [18] | ✓ | | ✓ | |
| Distributional Regularizers [3] | ✓ | | ✓ | ✓ |
| selective function [10] | | | | ✓ |
| attentive function [19] | ✓ | ✓ | ✓ | ✓ |

significant outputs, possibly producing insufficiently sparse representations [3]. Regularization strategy is an alternative approach: (i) L_1 -regularization refers to feature selection, which sets all unimportant features to zero [17] and is also a truncated sparse representation. (ii) L_2 -regularization is relatively smooth [18], and implicitly sparse like ReLU. (iii) Distributional Regularizers estimate the neural network output to a sparse distribution, which effectively ensures smooth sparsity [3], however it must rely on a prior distribution. As shown in Table I, we can conclude that a good sparse representation needs to satisfy four characteristics: learnable, non-prior, non-truncated and explicit. To learn an efficient sparse representation, we further propose attentive kernel-based VFA.

Attention mechanism can smoothly extract important features with normalized weights, which has been successfully applied in visual and machine translation tasks [20], [21]. In terms of emphasising local information, attention mechanism is consistent with sparse representation. Generally, attention mechanism encoding methods can be separated into hard-attention and soft-attention [19], which corresponds to two different sparsifications: truncated and non-truncated. Previously, Online Selective Kernel-based Temporal Difference (OSKTD) learning artificially defines a selective function to provide a truncated sparse representation [10], however it lacks adaptability and smoothness. To learn a non-truncated sparse representation, we focused on soft-attention and used the attentive function as the degree of sparsification. In addition, to guarantee stability of the online RL, we introduced two-timescale optimization [22] based on TD and propose Online Attentive Kernel-Based Temporal Difference (OAKTD) learning. Furthermore, we analyzed the convergence of OAKTD and compared it with existing methods on several control tasks. The experimental results verify that OAKTD is the best performing method.

The rest of this paper is organized as follows. Section II gives an introduction of the Markov Decision Process, kernel-based VFA and online dictionary construction, and selective kernel-based VFA. In Section III, we propose an

TABLE II
NOTATIONS.

| Symbol | Meaning |
|--|--|
| s, s' | states |
| $ s $ | dimensionality of state |
| a | an action |
| r | a reward |
| γ | discount rate |
| \mathcal{S} | set of all nonterminal states |
| $ \mathcal{S} $ | number of elements in set \mathcal{S} |
| \mathcal{R} | reward function |
| \mathcal{A} | set of all actions |
| \mathcal{D} | diagonal matrix of state distribution |
| π | policy (decision-making rule) |
| t | discrete time step |
| T | final time step of an episode |
| S_t, \hat{S}_t | states at time t |
| R_t | reward at time t |
| α_t, β_t | step-size at time t |
| $V^\pi(s)$ | value of state s under policy π (expected return) |
| $V^*(s)$ | value of state s under the optimal policy |
| $\theta, \theta_t, \bar{\theta}, \bar{\theta}_t$ | weights underlying an approximate value function |
| w, w_t | parameters of attentive function |
| \bar{w}, \bar{w}_t | parameters of attentive kernel-based VFA, $\bar{w}^\top = (w^\top, \bar{\theta}^\top)$, $\bar{w}_t^\top = (w_t^\top, \bar{\theta}_t^\top)$ |
| $V_\theta(s), V_{\theta, w}(s)$ | approximate value of state s given parameters θ, w |
| U_t | target for estimate at time t |
| $\phi(s)$ | feature vector of state s |
| $\phi_w(s)$ | feature vector of state s given parameter w |
| D | a fixed dictionary |
| $ D $ | number of dictionary vectors |
| D^* | stable dictionary |
| $ D^* $ | number of stable dictionary vectors |
| s_i | an element in dictionary D |
| $k(s, s_i)$ | kernel function |
| $\beta(s, s_i)$ | selective function |
| μ_1, μ_2 | thresholds |
| $a_w(s, s_i)$ | attentive function given parameter w |
| $\langle \cdot \rangle$ | tuple |
| \subset | subset of |
| \in | is an element of |
| $:=$ | equality relationship that is true by definition |
| W | a compact and convex subset $W \subset \mathbb{R}^{ \mathcal{S} + D }$ |
| Γ^W | a mapping that projects its argument into subset W |
| δ_t | temporal difference error at t |
| $\ \cdot\ $ | 2-norm |
| $\ X\ _{\mathcal{D}}$ | $\sqrt{X^\top \mathcal{D} X}$ |
| $\nabla_{\theta_t} V_\theta(S_t)$ | Jacobian of $V_\theta(S_t)$ at $\theta = \theta_t$ |

attentive kernel-based VFA and derive the OAKTD algorithm. In Section IV, we provide a stability analysis of OAKTD. Section V presents experimental settings, results and analysis. Finally, conclusions and future work are stated in Section VI.

II. BACKGROUND

A. Markov Decision Process

Consider a discounted Markov Decision Process (MDP) $\langle \mathcal{S}, \mathcal{A}, P, \mathcal{R}, \gamma \rangle$, where \mathcal{S} is a state space, \mathcal{A} is a finite action space, $\mathcal{R} : \mathcal{S} \times \mathcal{A} \times \mathcal{S} \rightarrow \mathbb{R}$ is a reward function, $P : \mathcal{S} \times \mathcal{A} \times \mathcal{S} \rightarrow [0, 1]$ is a state transition function and $\gamma \in (0, 1)$ is a discount factor [1]. A policy is a mapping $\pi : \mathcal{S} \times \mathcal{A} \rightarrow [0, 1]$, which defines for each action the selection probability conditioned on the state. The return at time t is defined as the discounted sum of rewards, which is then defined as

$$G_t := \sum_{i=1}^{\infty} \gamma^{i-1} R_{t+i}.$$

The infinite-horizon discounted value function given policy π is $V^\pi : \mathcal{S} \rightarrow \mathbb{R}$, which is then defined as

$$V^\pi(s) := \mathbb{E}[G_t | S_t = s, \pi].$$

The goal is to find an optimal policy $\pi^* = \arg \max_\pi V^\pi(s)$ to maximize the expectation of the discounted accumulative rewards in a long period. Under the optimal policy, the optimal value function $V^*(s)$ satisfies the Bellman optimality equation

$$V^*(s) = \max_{a \in \mathcal{A}} \mathbb{E}[r(s, a) + \gamma V^*(s') | s' \sim P(s, a, \cdot)],$$

where $r(s, a) = \mathbb{E}[R(s, a, s') | s' \sim P(s, a, \cdot)]$. For the large-scale or continuous state problems. Value Function Approximation (VFA) is a generalized method. An online RL algorithm requires low computational complexity. Thus, a common VFA for online RL is linear, which can be then defined as

$$V_\theta(s) = \theta^\top \phi(s) = \sum_{i=1}^m \theta_i \phi_i(s), \quad (1)$$

where $\phi(s) = (\phi_1(s), \dots, \phi_m(s))^\top \in \mathbb{R}^m$ is a feature vector, and $\theta = (\theta_1, \theta_2, \dots, \theta_m)^\top \in \mathbb{R}^m$ is a weight vector. Linear VFA can be quickly computed and possess elegant and sophisticated theoretical analysis, e.g., Temporal Difference with Gradient Correction (TDC) [6], Decentralized Temporal Difference Learning [7], Target-based Temporal Difference Learning [8] etc. However, their performances rely heavily on pre-defined feature functions. In nonlinear VFA, deep neural networks are effective at extracting state representations, but fail to be applied in online RL [2]. Another is kernel-based VFA, which will be introduced in the following subsection.

B. Kernel-based VFA and Online Dictionary Construction

Kernel-based value function is a memory-based and non-parametric model. According to Representer Theorem [23], the value function can be projected into the infinite-dimensional Reproducing Kernel Hilbert Spaces (RKHS), which is then defined as

$$V_\theta(s) = \theta^\top k(s) = \sum_{i=1}^{\infty} \theta_i k(s, s_i), \quad (2)$$

where kernel function $k : \mathcal{S} \times \mathcal{S} \rightarrow \mathbb{R}$ is a continuous, symmetric, and positive-definite function according to Mercer's theorem, e.g., a Gaussian kernel $k(s, s_i) = \exp(-\frac{\|s-s_i\|^2}{2\sigma^2})$. It is easy to find that the value function is impossible to use an infinite number of pairwise $\langle \theta_i, k(s, s_i) \rangle$ in (2). Therefore, kernel reduction for $\{\langle \theta_i, k(s, s_i) \rangle\}_\infty$ is indispensable in practice. The method of reduction is called dictionary construction. Kernel-based value function is then defined as

$$V_\theta(s) = \theta^\top k(s) = \sum_{s_i \in D} \theta_i k(s, s_i), \quad (3)$$

where D is a dictionary of states, the number of dictionary vectors $|D| \ll |\mathcal{S}|$, and learning parameters $\theta \in \mathbb{R}^{|D|}$.

Dictionary construction¹ is targeted at reducing infinite kernel function space [24], [10]. In fully online settings,

¹Dictionary construction is also known as kernel sparsification. To avoid confusion and to distinguish from sparse representations, we mainly use the term "dictionary construction" in this paper.

Modified Novelty Criterion (MNC) is a competitive method, as it can adaptively learn representation and provide lower computational complexity $O(n)$ compared with Approximation Linear Dependence (ALD) [10], [24]. The MNC is a distance-based dictionary construction method and the distance-based condition for a new feature vector $\phi(S_t)$ is

$$d_t = \min_{s_i \in D_{t-1}} \|\phi(s_i) - \phi(S_t)\|^2 \leq \mu_1, \quad (4)$$

where μ_1 is a threshold parameter. Using the kernel trick, by substituting $k(s_i, S_t)$ to $\phi(s_i)^\top \phi(S_t)$, we can obtain $d_t = \min_{s_i \in D_{t-1}} (k(s_i, s_i) - 2k(s_i, S_t) + k(S_t, S_t))$. Specially, we define $d_t = \min_{s_i \in D_{t-1}} (2 - 2k(s_i, S_t))$ with Gaussian kernel. The update rule for the sample dictionary D is then defined as

$$D_t = \begin{cases} D_{t-1}, & \text{if } d_t \leq \mu_1, \\ D_{t-1} \cup \{\phi(S_t)\}, & \text{otherwise.} \end{cases} \quad (5)$$

Online dictionary construction can ensure the feasibility of optimization with finite parameters, and enhances the generalization ability. However, some issues still exist in kernel-based VFA with online dictionary construction.

C. Sparse Representations for Kernel-based VFA

Catastrophic interference is one critical issue of VFA applied in online RL [3]. To formalize the interference in RL, the pairwise interference between two different samples has been proposed [2], which can be then defined as

$$PI(\theta_t, S_t, \hat{S}_t) := \mathcal{L}(\theta_{t+1}, \hat{S}_t | S_t) - \mathcal{L}(\theta_t, \hat{S}_t),$$

where S_t and \hat{S}_t are two different states. $\mathcal{L}(\theta_t, \hat{S}_t)$ is the objective function for the state \hat{S}_t . θ_{t+1} is updated by the gradient based state S_t . If PI is positive, the interference will occur. Under traditional TD algorithm, a natural loss function is the Mean Squared Value Error (MSVE), which is then defined as

$$\mathcal{L}(\theta) = \text{MSVE}(\theta) := \|V^\pi - V_\theta\|_{\mathcal{D}}^2,$$

where \mathcal{D} is the diagonal matrix of state distribution. The update of θ is

$$\theta_{t+1} = \theta_t + \alpha(U_t - V_{\theta_t}(S_t)) \nabla_{\theta_t} V_\theta(S_t),$$

where α is a step-size, U_t is target value and $\nabla_{\theta_t} V_\theta(S_t)$ is the Jacobian of $V_\theta(S_t)$ at $\theta = \theta_t$. Then, the pairwise interference in RL can be approximated by a Taylor expansion:

$$\begin{aligned} PI(\theta_t, S_t, \hat{S}_t) &\approx (\theta_{t+1} - \theta_t) \frac{\partial \mathcal{L}(\theta_t, \hat{S}_t)}{\partial \theta_t} \\ &= 2\alpha[U_t - V_{\theta_t}(S_t)][V^\pi(\hat{S}_t) - V_{\theta_t}(\hat{S}_t)] \nabla_{\theta_t} V_\theta(S_t)^\top \nabla_{\theta_t} V_\theta(\hat{S}_t). \end{aligned}$$

This equation provides some insights for interference analysis. It is difficult to determine whether interference occurs, because $V^\pi(\hat{S}_t)$ is unknown. Fortunately, we can avoid interference satisfying the condition $\nabla_{\theta_t} V_\theta(S_t)^\top \nabla_{\theta_t} V_\theta(\hat{S}_t) \rightarrow 0$. Furthermore, for a linear VFA, we have

$$\nabla_{\theta_t} V_\theta(S_t)^\top \nabla_{\theta_t} V_\theta(\hat{S}_t) = \phi(S_t)^\top \phi(\hat{S}_t),$$

where ϕ is feature vector. The condition can be also written as $\phi(S_t)^\top \phi(\hat{S}_t) \rightarrow 0$. Thus, to alleviate interference, sparse

representations can be an effective method to approximate the condition.

Similarly, in kernel-based VFA, we have

$$\nabla_{\theta_t} V_{\theta}(S_t)^\top \nabla_{\theta_t} V_{\theta}(\hat{S}_t) = \phi(S_t)^\top \phi(\hat{S}_t) = k(S_t, \hat{S}_t),$$

by the kernel trick. However, it is difficult for kernel-based VFA to guarantee an effective and explicit sparse representation in online RL, because the condition $k(S_t, \hat{S}_t) \rightarrow 0$ is hard to be satisfied. In order to encourage sparsification of kernel-based VFA, a selective kernel-based value function is proposed [10],

$$V(s) = \theta^\top K(s) \beta(s) = \sum_{s_i \in D} \theta_i k(s, s_i) \beta(s, s_i),$$

where $K(s)$ is the diagonal matrix of kernel function $k(s, s_i)$, and $\beta(s)$ is a distance-based selective function vector with elements $\beta(s, s_i)$, which is written as

$$\beta(s, s_i) = \begin{cases} 1, & k(s, s) - 2k(s, s_i) + k(s_i, s_i) < \mu_2, \\ 0, & \text{otherwise,} \end{cases}$$

where μ_2 is a threshold parameter. The selective function truncates partial kernels by a distance-based indicator function and can also be replaced by other sparse representations in structures. Two simple examples of this will be provided. In dropout, we have

$$\beta_{\text{dropout}}(s, s_i) = \begin{cases} 1, & \text{with } \eta \text{ possibility,} \\ 0, & \text{otherwise,} \end{cases}$$

where $0 < \eta < 1$. Similarly, for ReLU, we have

$$\beta_{\text{ReLU}}(s, s_i) = \begin{cases} 1, & k(s, s_i) > b, \\ 0, & \text{otherwise,} \end{cases}$$

where b is a learnable bias. In online RL, selective kernel-based VFA provides a generalized framework for combining several existing sparse methods. However, as mentioned previously, these methods may exhibit problems in their learnable, non-prior, non-truncated and explicit characteristics. Therefore, we will introduce the attentive function in greater detail in the next section.

III. ONLINE ATTENTIVE KERNEL-BASED TEMPORAL DIFFERENCE LEARNING

The highlights of our methods are: (i) we designed an attentive kernel-based value function, (ii) we adopted online two-timescale optimization. In the following part, details of Online Attentive Kernel-Based Temporal Difference learning are presented.

A. Attentive Kernel-based VFA

In order to obtain a good sparse representation, we introduce an attentive function. As shown in Fig. 1, based on the

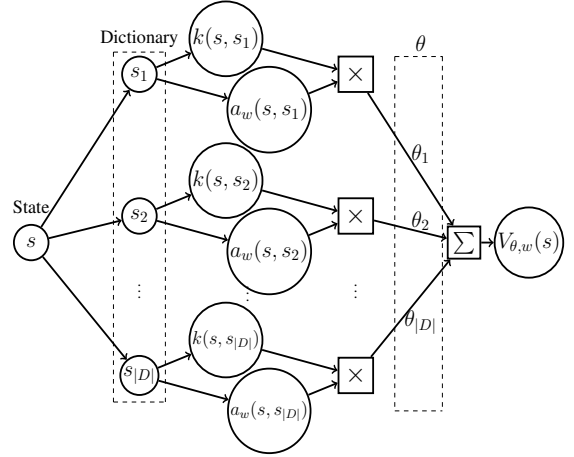


Fig. 1. Attentive Kernel-based VFA. $D = \{s_1, s_2, \dots, s_{|D|}\}$ is a fixed dictionary, and the multiplication of $k(s, \cdot)$ and $a_w(s, \cdot)$ is used as a sparse representation.

framework of sparse representation for kernel-based VFA, we have attentive kernel-based value function²

$$V_{\theta,w}(s) = \theta^\top K(s) a_w(s) = \sum_{s_i \in D} \theta_i k(s, s_i) a_w(s, s_i), \quad (6)$$

where $K(s)$ is the diagonal matrix of kernel function $k(s, s_i)$, parameters w and θ are learning parameter vectors, and $a_w(s)$ is the attentive function vector with elements $a_w(s, s_i)$. D is a dictionary constructed online by MNC.

Our model uses the attentive function as the degree of sparsification. Based on the generalized attention model, we defined a novel score function based on L_1 Norm

$$e(s, s_i) = w^\top \psi(s, s_i), \quad (7)$$

where the learning parameter $w \in \mathbb{R}^{|s|}$, and $\psi(s, s_i) \in \mathbb{R}^{|s|}$ is the vector with the k -th element $|\chi_k(s) - \chi_k(s_i)|$, where $\chi_k(s)$ is the k -th element of state s . After normalization by the softmax function, the attentive function is then defined as

$$a_w(s, s_i) = \frac{\exp(w^\top \psi(s, s_i))}{\sum_{s_j \in D} \exp(w^\top \psi(s, s_j))}. \quad (8)$$

Attentive kernel-based VFA is nonlinear, which may lead to algorithm instability. Thus, we introduced two-timescale optimization to alleviate this issue in the next subsection.

B. Two-Timescale Optimization

To guarantee stability of attentive kernel-based VFA, we adopt two-timescale optimization [22], which in process was divided into slow and fast parts. As shown in Fig. 2, the slow part uses an auxiliary parameter $\bar{\theta}$ to learn attentive kernel-based sparse features ϕ_w and the fast part approximates a linear value function $V_{w,\bar{\theta}}$ with the learned features. In structure, two-timescale optimization splits attentive kernel-based VFA into two parts: attentive sparse representation

²For convenience of expression, we use $V_{\theta,w}$ to replace $V_{\theta,w,D}$, which is online attentive kernel-based VFA about dictionary D . In subsequent theoretical proofs, we take dictionary convergence into account and re-add the dictionary symbol, e.g., $\Phi_{w,D}$.

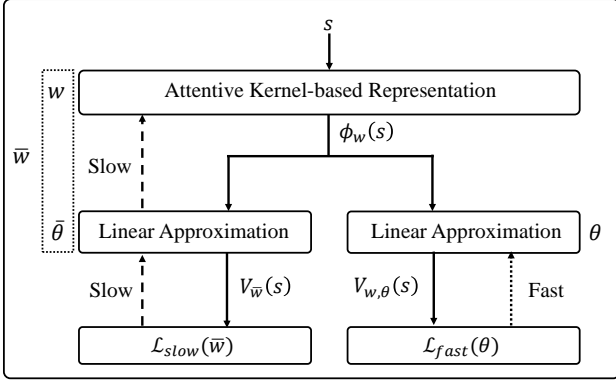


Fig. 2. Two-timescale optimization. The left is a slow learning process, where $\bar{\theta}$ is an auxiliary learning parameter and $\bar{w}^\top = (w^\top, \bar{\theta}^\top)$. The right is a fast learning process and the dotted line shows the loss backpropagation.

and linear approximation. Then, attentive kernel-based value function can be also written as

$$V_{\theta,w}(s) = \theta^\top \phi_w(s),$$

where $\phi_w(s) = K(s)a_w(s)$ is attentive kernel-based features. In slow process, to obtain a stable attentive kernel-based representation learning, we use Mean Squared Bellman Error (MSBE) as objective function, which can be written as

$$\begin{aligned} \text{MSBE}(\bar{w}) &= \|\mathbb{T}V_{\bar{w}} - V_{\bar{w}}\|_{\mathcal{D}}^2 \\ &= \sum_{s \in \mathcal{S}} d(s) (\mathbb{E}[\delta_t | S_t = s])^2, \end{aligned}$$

where $\bar{w}^\top = (w^\top, \bar{\theta}^\top)$ are learning parameters, \mathbb{T} is known as Bellman operator, $\delta_t = R_{t+1} + \gamma V_{\bar{w}_t}(S_{t+1}) - V_{\bar{w}_t}(S_t)$ is one-step TD error, $d(s)$ is distribution of state s , $\sum_{s \in \mathcal{S}} d(s) = 1$, and \mathcal{D} is a diagonal matrix of $d(s)$. Generally, in residual-gradient algorithm, Bellman error for a state is expected TD error in that state [25]. To get an unbiased estimate for MSBE, double sampling of subsequent states is required. However, in online interaction with an environment, this would seem be impossible. Thus, we adopt naive residual-gradient based on the Mean Squared Temporal Difference Error (MSTDE), $\sum_{s \in \mathcal{S}} d(s) \mathbb{E}[\delta_t^2 | S_t = s]$ [1], and the objective function in slow process is defined as

$$\mathcal{L}_{slow}(\bar{w}) = \sum_{s \in \mathcal{S}} d(s) (r + \gamma V_{\bar{w}}(s') - V_{\bar{w}}(s))^2,$$

For a nonlinear VFA, the update of slow part is generally by a projection operator described as

$$\bar{w}_{t+1} = \Gamma^W \left(\bar{w}_t + \alpha_t \delta_t (\nabla_{\bar{w}_t} V_{\bar{w}}(S_t) - \gamma \nabla_{\bar{w}_t} V_{\bar{w}}(S_{t+1})) \right), \quad (9)$$

where α_t is a step-size, $\nabla_{\bar{w}_t} V_{\bar{w}}(s) \in \mathbb{R}^{|s|+|D|}$ is the Jacobian of $V_{\bar{w}}(s)$ at $\bar{w} = \bar{w}_t$, and Γ^W is a mapping that projects its argument into an appropriately chosen compact convex subset $W \subset \mathbb{R}^{|s|+|D|}$ with a smooth boundary³.

³The purpose of this projection is to prevent the parameters to diverge in the initial phase of the nonlinear approximation. It is very likely that no projections will take place at all if one selects W large enough [26]. One of the main reason for the projection is to facilitate convergence analysis.

Furthermore, we deduce the update formula based on gradient in terms of their respective components. For a linear FA, we have

$$\begin{aligned} \bar{\theta}_{t+1} &= \Gamma^W \left(\bar{\theta}_t + \alpha_t \delta_t (\nabla_{\bar{\theta}_t} V_{\bar{w}}(S_t) - \gamma \nabla_{\bar{\theta}_t} V_{\bar{w}}(S_{t+1})) \right) \\ &= \Gamma^W \left(\bar{\theta}_t + \alpha_t \delta_t (K(S_t)a_{w_t}(S_t) - \gamma K(S_t)a_{w_t}(S_{t+1})) \right). \end{aligned} \quad (10)$$

In a representation learning, we can obtain the same update of w_{t+1} , which is written as

$$\begin{aligned} w_{t+1} &= \Gamma^W \left(w_t + \alpha_t \delta_t (\nabla_{w_t} V_{\bar{w}}(S_t) - \gamma \nabla_{w_t} V_{\bar{w}}(S_{t+1})) \right) \\ &= \Gamma^W \left(w_t + \alpha_t \delta_t (\nabla_{w_t} \phi_w^\top(S_t) - \gamma \nabla_{w_t} \phi_w^\top(S_{t+1})) \bar{\theta}_t \right), \end{aligned} \quad (11)$$

where $\nabla_{w_t} \phi_w^\top(s) \in \mathbb{R}^{|s| \times |D|}$ is the Jacobian of $\phi_w^\top(s)$ at $w = w_t$, and $\nabla_{w_t} \phi_w(s, s_i) = k(s, s_i) \nabla_{w_t} a_{w_t}(s, s_i)$ is the column corresponding to s_i . For convenience, we define

$$\begin{aligned} \dot{a}_{w_t}(s, s_i) &:= \nabla_{w_t} a_{w_t}(s, s_i) \\ &= \frac{\nabla_{w_t} e(s, s_i) \exp(e(s, s_i))}{\sum_{s_j \in \mathcal{D}} \exp(e(s, s_j))} - \\ &\quad \frac{\exp(e(s, s_i)) \sum_{s_j \in \mathcal{D}} \nabla_{w_t} e(s, s_j) \exp(e(s, s_j))}{\sum_{s_j \in \mathcal{D}}^2 \exp(e(s, s_j))} \\ &= a_{w_t}(s, s_i) \left[\psi(s, s_i) - \frac{\sum_{s_j \in \mathcal{D}} \psi(s, s_j) \exp(e(s, s_j))}{\sum_{s_j \in \mathcal{D}} \exp(e(s, s_j))} \right] \\ &= a_{w_t}(s, s_i) \left[\psi(s, s_i) - \sum_{s_j \in \mathcal{D}} a_{w_t}(s, s_j) \psi(s, s_j) \right]. \end{aligned}$$

Then, the updating of w_{t+1} in (11) can be rewritten as

$$\begin{aligned} w_{t+1} &= \Gamma^W \left(w_t + \beta_t \delta_t \sum_{s_i \in \mathcal{D}} \bar{\theta}_{i,t} (k(S_t, s_i) \dot{a}_{w_t}(S_t, s_i) - \right. \\ &\quad \left. \gamma k(S_{t+1}, s_i) \dot{a}_{w_t}(S_{t+1}, s_i)) \right). \end{aligned} \quad (12)$$

After attentive kernel-based representation learning, a linear state value estimate is available. In fast process, a natural objective function can use the Mean Squared Value Error (MSVE) which measures the difference between the approximate value $V_{\theta,w}$ and the true value V^π [1], which is defined as

$$\begin{aligned} \mathcal{L}_{fast}(\theta) &= \|V^\pi - V_{\theta,w}\|_{\mathcal{D}}^2 \\ &= \sum_{s \in \mathcal{S}} d(s) [V^\pi(s) - V_{\theta,w}(s)]^2. \end{aligned}$$

Because V^π is unknown, a prototypical semi-gradient method uses $U_t = R_{t+1} + \gamma V_{\theta_t, w_t}(S_{t+1})$ as its target in place of $V^\pi(S_t)$ after calculating its gradient, and the update of the fast is defined as

$$\begin{aligned} \theta_{t+1} &= \theta_t + \beta_t (U_t - V_{\theta_t, w_t}(S_t)) \nabla_{\theta_t} V_{\theta_t, w_t}(S_t) \\ &= \theta_t + \beta_t \delta_t K(S_t) a_{w_t}(S_t), \end{aligned} \quad (13)$$

where β_t is a fast learning step-size, satisfying $\frac{\alpha_t}{\beta_t} \rightarrow 0$ as $t \rightarrow \infty$.

C. Algorithm Description

Our proposed OAKTD is an online learning algorithm, which aims to enhance accuracy and stability of kernel-based algorithms. The main steps of OAKTD include three aspects: (i) Online dictionary construction; (ii) Attentive kernel-based representation learning; (iii) Linear value function evaluation.

Our OAKTD is based on traditional RL paradigm and the classical framework of on-policy TD. The MNC-based dictionary construction is a distance-based method with a finite number of dictionary vectors which appeals to Theorem 2.1, Chapter 2.2 of Engle [27], [28]. Additionally, we can adjust threshold μ_1 and enhance the exploration to make the dictionary converge at a very fast speed. As result, the dictionary convergence time was short and negligible. Then, we calculated the computational complexity in OAKTD using $n + n^2 + nm$, where $n = |D^*|$ is the number of stable dictionary vectors and $m = |s|$ is state's dimension. In reality, the state's dimension is generally far less than the dictionary size $m \ll n$, the real computational complexity of each update of OAKTD is $O(n^2)$. In summary, pseudocode for the OAKTD is summarized as Algorithm 1.

Algorithm 1 Online Attentive Kernel-Based Temporal Difference Learning

- 1: Input: the policy π to be evaluated
 - 2: Algorithm parameter: $\alpha, \beta, \epsilon, \mu_1$
 - 3: Initialize parameters $D = \emptyset, \theta, \bar{\theta}, w$
 - 4: **Loop** for each episode:
 - 5: initialize state s
 - 6: **Loop** for each step of episode:
 - 7: Sample $a \sim \pi(s, \cdot)$
 - 8: Take action a , observe r, s'
 - 9: Update dictionary D according to (5)
 - 10: Update $\bar{\theta}, w$ according to (10), (12)
 - 11: Update θ according to (13)
 - 12: Update learning rate α, β and greedy rate ϵ
 - 13: $s \leftarrow s'$
 - 14: **Until** s is terminal
-

IV. THE STABILITY ANALYSIS OF OAKTD

In this section, we analyze the convergence of online dictionary construction, and the convergence of two-timescale optimization under a fixed dictionary assumption and other standard assumptions.

Assumption 1: The kernel function k in dictionary construction is a Lipschitz continuous Mercer kernel and state space \mathcal{S} is a compact subset of a Banach space.

Theorem 1 (Convergence of MNC-based Dictionary Construction): Let Assumption 1 hold. Under MNC-based dictionary construction procedure, for any training sequence $\{s_i\} \in \mathcal{S}(i = 1, 2, \dots, \infty)$ and any $\mu_1 > 0$, the number of dictionary vectors is finite, and the dictionary sequence $\{D_t\}_{t \in \mathbb{N}}$ converges to a stable dictionary $D^* \subset \mathcal{S}$.

Proof: According to Assumption 1, we claim that for any training sequence $\{s_i\} \in \mathcal{S}(i = 1, 2, \dots, \infty)$ and for any $\mu_1 > 0$, the number of dictionary vectors is finite, and the

dictionary sequence $\{D_t\}_{t \in \mathbb{N}}$ converges to a stable dictionary $D^* \subset \mathcal{S}$. According to the MNC-based dictionary construction (5), it is easy to find that any two elements $\phi(s_i)$ and $\phi(s_j)$ in the dictionary are $\sqrt{\mu_1}$ -separated, satisfying $\|\phi(s_i) - \phi(s_j)\| > \sqrt{\mu_1}$. Then, based on the analysis given by Theorem 2.1 and Proposition 2.2, Chapter 2.2 of Engle [27], [28], the claim follows. ■

We consider a function $\Gamma : U \subseteq \mathbb{R}^{d_1} \rightarrow X \subseteq \mathbb{R}^{d_2}$ is Frechet differentiable at $x \in U$, i.e., there exists a bounded linear operator $\hat{\Gamma}_x : \mathbb{R}^{d_1} \rightarrow \mathbb{R}^{d_2}$ such that the limit

$$\hat{\Gamma}_x(y) = \lim_{\epsilon \downarrow 0} \frac{\Gamma(x + \epsilon y) - \Gamma(x)}{\epsilon}.$$

Recall that Γ^W is the projection onto a prescribed compact and convex subset $W \subset \mathbb{R}$, where $\Gamma^W(x) = x$, for $x \in \overset{\circ}{W}$, $\overset{\circ}{W}$ is the interior of W , while for $x \notin \overset{\circ}{W}$, it is the nearest point in W w.r.t. the Euclidean distance $\Gamma^W(x) = \arg \min_{x' \in W} \|x' - x\|$. Then, the above limit exists when the boundary ∂W of W is smooth. Further, for $x \in \overset{\circ}{W}$, we have

$$\hat{\Gamma}_x^W(y) = \lim_{\epsilon \rightarrow 0} \frac{\Gamma^W(x + \epsilon y) - x}{\epsilon} = \lim_{\epsilon \rightarrow 0} \frac{x + \epsilon y - x}{\epsilon} = y.$$

i.e., $\hat{\Gamma}_x^W(\cdot)$ is an identity map for $x \in \overset{\circ}{W}$.

Assumption 2: The Markov chain induced by the given policy π is ergodic, i.e., aperiodic and irreducible.

Assumption 3: Given a realization of the transition dynamics of the MDP in the form of a sample trajectory $\mathcal{O}_\pi = \{S_0, A_0, R_1, A_1, R_2, S_2, \dots\}$, where the initial state $S_0 \in \mathcal{S}$ is chosen arbitrarily, while the action $A_t \sim \pi(S_t, \cdot)$, the transitioned state $S_{t+1} \sim P(S_t, A_t, \cdot)$ and the reward $R_{t+1} = r(S_t, A_t, S_{t+1})$.

Assumption 4: The pre-determined, deterministic, step-size sequences $\{\alpha_t\}_{t \in \mathbb{N}}$ and $\{\beta_t\}_{t \in \mathbb{N}}$ satisfy $\alpha_t, \beta_t \in (0, 1]$, $\sum_{t=0}^{\infty} \alpha_t = \sum_{t=0}^{\infty} \beta_t = \infty$, $\sum_{t=0}^{\infty} \alpha_t^2 < \infty$, $\sum_{t=0}^{\infty} \beta_t^2 < \infty$ and $\lim_{t \rightarrow \infty} \frac{\alpha_t}{\beta_t} = 0$.

Note that $\lim_{t \rightarrow \infty} \frac{\alpha_t}{\beta_t} = 0$ implies that $\{\alpha_t\}$ converges to 0 relatively faster than $\{\beta_t\}$. The purpose of using different learning rates is to form a quasi-stationary estimate [29]. When viewed from the faster timescale recursion, the slower timescale recursion seems quasi-static. When viewed from the slower timescale, the faster timescale recursion seems equilibrated. While analyzing the asymptotic behaviour of the relatively faster timescale stochastic recursion, it is analytically admissible to consider the slow timescale stochastic recursion to be quasi-stationary [6], [22].

Theorem 2 (Convergence of Two-Timescale Optimization): Let Assumptions 2-4 hold. Let $D \subset \mathcal{S}$ is a fixed dictionary. Let $\bar{w}^\top = (w^\top, \bar{\theta}^\top)$ and Γ^W is a projection to a compact, convex subset $W \subset \mathbb{R}^{|s|+|D|}$ with smooth boundary. Let Γ^W be Frechet differentiable and $\hat{\Gamma}_{\bar{w}}^W(-\frac{1}{2}\nabla_{\bar{w}}\mathcal{L}_{slow})(\bar{w})$ be Lipschitz continuous. Let \mathcal{W} be the set of asymptotically stable equilibria of the following Ordinary Differential Equation (ODE) contained inside W :

$$\frac{d}{dt}\bar{w}(t) = \hat{\Gamma}_{\bar{w}(t)}^W(-\frac{1}{2}\nabla_{\bar{w}}\mathcal{L}_{slow})(\bar{w}(t)), \quad (14)$$

where $\bar{w}(0) \in \overset{\circ}{W}$ and $t \in \mathbb{R}_+$. Then the stochastic sequeue $\{\bar{w}_t\}_{t \in \mathbb{N}}$ generated by natural residual-gradient algorithm

within the two-timescale optimization converges almost surely to \mathcal{W} . Furthermore, the stochastic sequence $\{\theta_t\}_{t \in \mathbb{N}}$ generated by semi-gradient algorithm within the two-timescale setting converges almost surely to the limit θ^* , which satisfies

$$\Phi_{\bar{w}^*, D} \theta^* = \Pi_{\bar{w}^*, D} \mathbb{T}(\Phi_{\bar{w}^*, D} \theta^*), \quad (15)$$

where $\bar{w}^* \in \mathcal{W}$, $\Phi_{\bar{w}^*, D}$ is the attentive kernel-based feature matrix with the $\phi_{\bar{w}^*, D}(s)$ as its rows, and $\Pi_{\bar{w}^*, D}$ is a projection operator according to $\Pi_{\bar{w}^*} V = \arg \min_{\bar{V} \in \mathcal{F}} \|\bar{V} - V\|_D^2$ with $\mathcal{F} = \{\Phi_{\bar{w}^*, D} \theta\}$.

Proof: The proof is very similar to that given by two-timescale networks [22]. In particular, we assume that the dictionary is fixed, which is to avoid the disturbance caused by dictionary construction [30].

In the slow optimization process, to analyze the behaviour of the slow optimization, we apply the ODE-based analysis of stochastic recursive algorithms [31], [32]. The ODE-based analysis is elegant, conclusive and further guarantees that limit points of the stochastic recursion will almost surely belong to the compact internally connected chain transitive invariant set of the equivalent ODE.

Define the filtration $\{\mathcal{F}_t\}_{t \in \mathbb{N}}$, a family of increasing natural σ -fields, where $\mathcal{F}_t \doteq \sigma(\{\bar{w}_i, S_i, R_i; 0 < i < t\})$. Then, we recall the previous projected stochastic recursion updating \bar{w} , which can be rewritten as

$$\bar{w}_{t+1} = \Gamma^W(\bar{w}_t + \alpha_t(h(\bar{w}_t) + M_{t+1} + l_t)), \quad (16)$$

where $h(\bar{w}_t) \doteq \mathbb{E}[\delta_t(\nabla_{\bar{w}_t} V_{\bar{w}}(S_t) - \gamma \nabla_{\bar{w}_t} V_{\bar{w}}(S_{t+1}))]$, the noise term $M_{t+1} \doteq \delta_t(\nabla_{\bar{w}_t} V_{\bar{w}}(S_t) - \gamma \nabla_{\bar{w}_t} V_{\bar{w}}(S_{t+1})) - \mathbb{E}[\delta_t(\nabla_{\bar{w}_t} V_{\bar{w}}(S_t) - \gamma \nabla_{\bar{w}_t} V_{\bar{w}}(S_{t+1}) | \mathcal{F}_t]$ and the bias $l_t \doteq \mathbb{E}[\delta_t(\nabla_{\bar{w}_t} V_{\bar{w}}(S_t) - \gamma \nabla_{\bar{w}_t} V_{\bar{w}}(S_{t+1}) | \mathcal{F}_t] - h(\bar{w}_t)$.

Further,

$$\begin{aligned} \bar{w}_{t+1} &= \bar{w}_t + \alpha_t \frac{\Gamma^W(\bar{w}_t + \alpha_t(h(\bar{w}_t) + M_{t+1} + l_t) - \bar{w}_t)}{\alpha_t} \\ &= \bar{w}_t + \alpha_t \left(\hat{\Gamma}_{\bar{w}_t}^W(h(\bar{w}_t)) + \hat{\Gamma}_{\bar{w}_t}^W(M_{t+1}) \right. \\ &\quad \left. + \hat{\Gamma}_{\bar{w}_t}^W(l_t) + o(\alpha_t) \right), \end{aligned} \quad (17)$$

where Γ^W and $\hat{\Gamma}_{\bar{w}_t}^W$ are defined in previous section.

Then, a few observations are in order: (i) $\hat{\Gamma}_{\bar{w}_t}^W(h(\bar{w}_t))$ is a Lipschitz continuous function in \bar{w}_t , which follows from the hypothesis of the Theorem. (ii) $\hat{\Gamma}_{\bar{w}_t}^W(M_{t+1})$ is a truncated martingale difference noise. Indeed, it is easy to verify that the noise sequence $\{M_{t+1}\}_{t \in \mathbb{N}}$ is a martingale-difference sequence with respect to the filtration $\{\mathcal{F}_t\}_{t \in \mathbb{N}}$, i.e., $\forall t \in \mathbb{N}$, M_{t+1} is \mathcal{F}_{t+1} -measurable and integrable, and $\mathbb{E}[M_{t+1} | \mathcal{F}_t] = 0$ a.s., $\forall t \in \mathbb{N}$. Also, since $\hat{\Gamma}_{\bar{w}_t}^W$ is a bounded linear operator, we have $\hat{\Gamma}_{\bar{w}_t}^W(M_{t+1})$ to be \mathcal{F}_{t+1} -measurable and integrable, $\forall t \in \mathbb{N}$. Further, $\exists K_0 \in (0, \infty)$, such that

$$\mathbb{E} \left[\|\hat{\Gamma}_{\bar{w}_t}^W(M_{t+1})\|^2 | \mathcal{F}_t \right] \leq K_0(1 + \|\bar{w}_t\|^2) \quad a.s.,$$

which follows directly from the finiteness of the Markov chain [33] and the boundary ∂W is smooth. (iii) For the bias, we have

$$\begin{aligned} \|\hat{\Gamma}_{\bar{w}_t}^W(l_t)\| &= \left\| \lim_{\epsilon \rightarrow 0} \frac{\Gamma^W(\bar{w}_t + \epsilon l_t) - \Gamma^W(\bar{w}_t)}{\epsilon} \right\| \\ &\leq \lim_{\epsilon \rightarrow 0} \frac{\|\Gamma^W(\bar{w}_t + \epsilon l_t) - \Gamma^W(\bar{w}_t)\|}{\epsilon} \\ &\leq \lim_{\epsilon \rightarrow 0} \frac{\|\bar{w}_t + \epsilon l_t - \bar{w}_t\|}{\epsilon} = \|l_t\|, \end{aligned}$$

and $\hat{\Gamma}_{\bar{w}_t}^W(l_t) \rightarrow 0$ as $t \rightarrow \infty$ a.s., which follows directly from the ergodicity and finiteness of the underlying Markov chain [33]. (iv) $o(\alpha_t) \rightarrow 0$ as $t \rightarrow \infty$. (v) The iterates of \bar{w}_t remain bounded a.s., i.e.,

$$\sup_{t \in \mathbb{N}} \|\bar{w}_t\| < \infty, \quad a.s.,$$

since $\bar{w}_t \in W, \forall t \in \mathbb{N}$ and W is compact.

Thus, by appealing to Theorem 2, Chapter 2 of Borkar [32], we conclude that the stochastic recursion (11) converges to the asymptotically stable equilibria of the ODE constrained inside W , which is

$$\frac{d}{dt} \bar{w}(t) = \hat{\Gamma}_{\bar{w}(t)}^W(h(\bar{w}_t)) = \hat{\Gamma}_{\bar{w}(t)}^W(-\frac{1}{2} \nabla_{\bar{w}} \mathcal{L}_{slow})(\bar{w}(t)),$$

where $\bar{w}(0) \in \dot{W}$ and $t \in \mathbb{R}_+$.

In the fast optimization process, the fast optimization is a traditional TD algorithm, our point of interest for the on-policy algorithm. Stability analysis of on-policy TD has been given by Sutton [1], which converges to a TD fixed point. Further, we obtain a fixed point given a stable $\bar{w}_t \equiv \bar{w}^*$, which follows from the TD fixed point of the fast optimization

$$\Phi_{\bar{w}^*, D} \theta^* = \Pi_{\bar{w}^*, D} \mathbb{T}(\Phi_{\bar{w}^*, D} \theta^*),$$

which is the final fixed point of two-timescale optimization. \blacksquare

We prove that the online dictionary construction is convergent, and the two-timescale optimization is convergent under the assumption that the dictionary is fixed. Our analysis is not enough to guarantee that the OAKTD algorithm is convergent. However, this analysis is acceptable, because under the assumption that the dictionary construction converges first, i.e., after the dictionary is fixed, the convergence of OAKTD is guaranteed. We will verify this assumption in the next section.

V. EXPERIMENTS

In this section, we conduct experiments on four classic control tasks with continuous state spaces: Mountain Car, Acrobot, CartPole and Puddle World [11], [1], which are all public benchmarks for studying online reinforcement learning algorithms. To accurately evaluate performance of the attentive kernel-based model as sparse representation, we compared our proposed OAKTD⁴ with OKTD, OSKTD and TD with Tile Coding. In addition, to reflect characteristics of the attention mechanism as a degree of sparsification, we representatively visualize the attention on the kernel in Mountain Car since it is a 2-dimensional task similar to Puddle World.

⁴Note that OAKTD is a learning algorithm for prediction. In this paper, we use its on-policy version to learn for control, and adopt ϵ -greedy policy. But we still use the abbreviation OAKTD rather than OAK-SARSA.

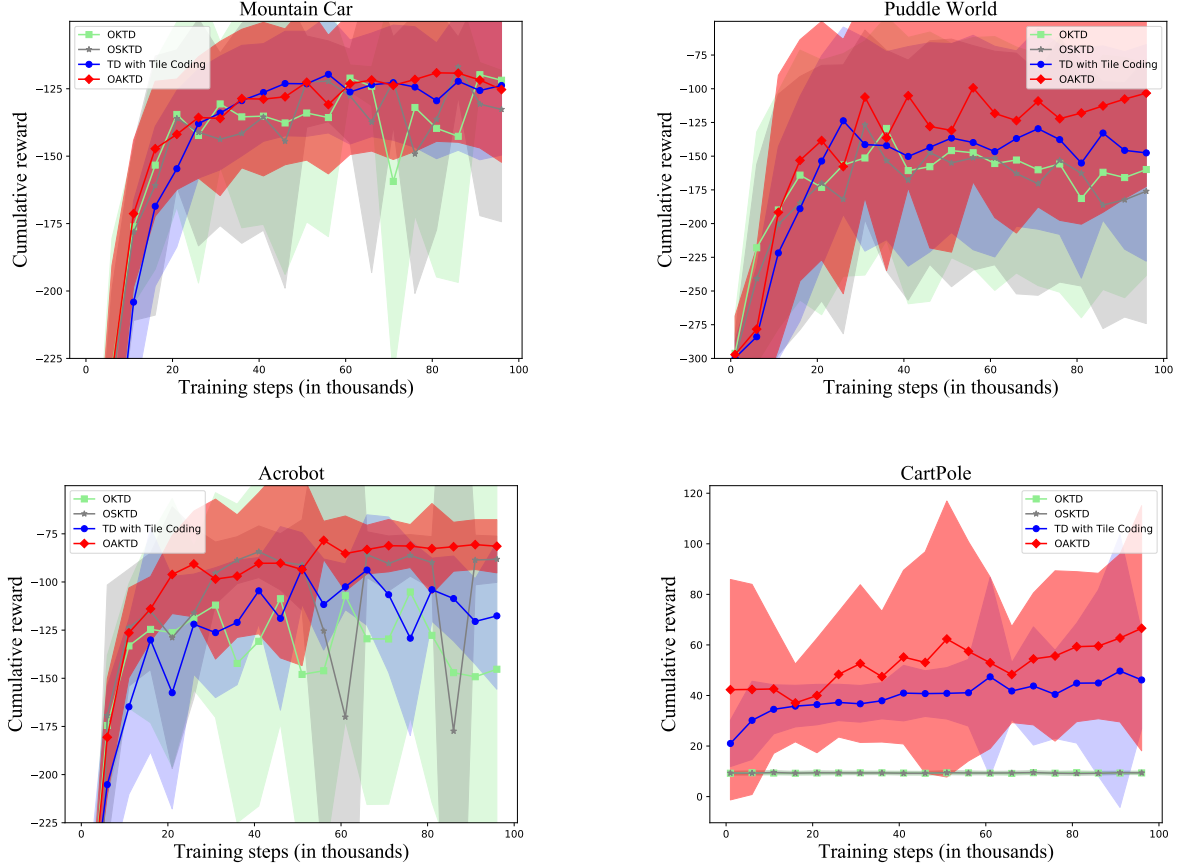


Fig. 3. Learning curves in Mountain Car, Acrobot, CartPole and Puddle World. The abscissa is the number of training steps, and the ordinate is the cumulative reward.

A. Descriptions of Control Tasks

The Mountain Car is the problem about how to drive an car up to the top of a hill. The difficulty is that gravity is much stronger than the car’s engine and thus the car cannot accelerate directly to up the hill. There are three alternative actions: full throttle forward (+1), full throttle reverse (−1), and zero throttle (0). Its position x_{t+1} can be updated by its last position x_t and velocity \dot{x}_t , which is,

$$x_{t+1} = \text{bound}[x_t + \dot{x}_t],$$

where $\dot{x}_{t+1} = \text{bound}[\dot{x}_t + 0.001a_t - 0.0025 \cos(3x_t)]$, the bound operation enforces $-1.2 \leq x_{t+1} \leq 0.5$ and $-0.07 \leq \dot{x}_{t+1} \leq 0.07$. In addition, when x_{t+1} reaches the left bound, \dot{x}_{t+1} will be reset to zero. The reward is -1 for all states except the goal state at the top of the hill in which the episode ends with a reward 0. The discount factor is set to 0.99, and each episode starts from a random position $x_0 \in [-0.6, -0.4]$ with zero velocity.

The Acrobot is a two-link under-actuated robot. Our goal is to swing the end-effector at a height at least the length of one link above the base. There are also three discrete actions: apply positive torque (1), apply negative torque (−1), and apply no torque (0). The state consists of the two rotational joint angles and their velocities. The reward is -1 for all the states except the goal state in which the episode ends with a reward 0. The

discount factor is set to 0.99. The agent is initialized in a downward vertical position.

The Cartpole is a the classic inverted pendulum problem with a center of gravity above its pivot point. It is unstable and can be controlled by moving the pivot point under the center of mass. The state of Cartpole consists of its position, velocity, angle, and angular velocity. The cart only has two possible actions: move to the left or move to the right. A reward of +1 is provided for every timestep that the pole remains upright. The discount factor is set to 1. The goal is to keep the cartpole balanced by applying appropriate forces to a pivot point.

The Puddle World is a task to seek for a goal position in a limited scene. The environment is a 1×1 square, where the puddles are 0.1 in radius and are located at center points (0.1, 0.75) to (0.45, 0.75) and (0.45, 0.4) to (0.45, 0.8). The agent starts at position (0.2, 0.4) and can choose five actions, up, down, left, right and stop, which moved approximately 0.05 in these directions under the boulder $[0, 1]$. In addition, a random gaussian noise with standard deviation 0.01 was also added to the motion along both dimensions. The reward is -1 for each time step plus additional penalties if the agent does not enter the puddles. These penalties were -400 times the distance to the nearest edge of the puddles regions. The discount factor is set to 0.999.

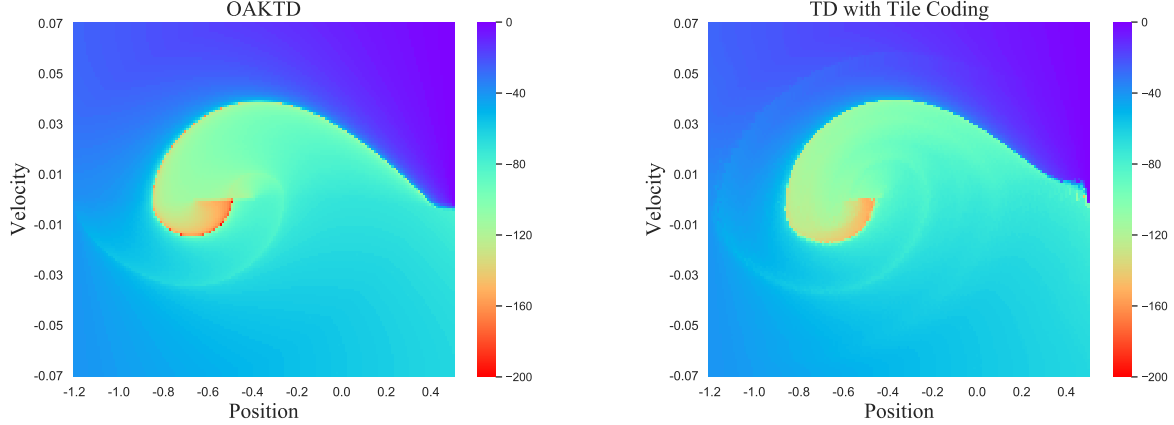


Fig. 4. Visualized in the color images are rewards on the whole state space. The left shows the performance of OAKTD and the right shows the performance of TD with Tile Coding.

B. Experimental Settings

In the Mountain Car task, for fair comparison as possible, we adopt ϵ -greedy exploration in the learning process, and set the greedy parameter ϵ to $\epsilon_t = 0.9999^t$, i.e., it will gradually decreases to zero as those methods proceed. The learning rate of linear approximation is uniformly set to 0.01×0.999999^t , which is also the fast learning rate in OAKTD. In online kernel-based methods, we use a Gaussian kernel with parameter $\sigma_2 = 1$. It is necessary to standardize the states for eliminating the effect of feature scale, and the k -th element can be defined as $\frac{\chi_k(s) - \min(\chi_k(s))}{\max(\chi_k(s)) - \min(\chi_k(s))}$. Then, the parameters of online dictionary construction are set to $\mu_1 = 0.1$, $\sigma_1 = 1$. For the specific parameters of different methods, we set to the slow learning rate $\alpha_t = 0.05 \times 0.99999^t$, the fast learning rate $\beta_t = 0.01 \times 0.999999^t$. In OSKTD, we set to selective function $\mu_2 = 1$. In addition, in TD with Tile Coding. we set the number of tilings to 16, the size of every tiling to 256.

In the Acrobot task, the learning rate is uniformly set to 0.001×0.999999^t . For online kernel-based methods, the parameters of dictionary construct are set to $\mu_1 = 0.3$, $\sigma_1 = 1$ and the parameter of kernel function is set to $\sigma_2 = 1$. For the specific parameters of different methods, we set to the slow learning rate $\alpha_t = 0.1 \times 0.99999^t$, the fast learning rate $\beta_t = 0.001 \times 0.999999^t$ in OAKTD. In OSKTD, we set selective function to $\mu_2 = 1$. In addition, in TD with Tile Coding. we set the number of tilings to 16, the size of every tiling to 4096.

In the CartPole task, the learning rate is uniformly set to 0.01×0.9999999^t . The parameters of dictionary construct are same as the setting of the Acrobot. For the specific parameters of different methods, in OAKTD, we set to the slow learning rate $\alpha_t = 0.1 \times 0.999999^t$ and the fast learning rate $\beta_t = 0.01 \times 0.9999999^t$. In OSKTD, we set to selective function $\mu_2 = 1$. In addition, in TD with Tile Coding, we set the number of tilings to 16, the size of every tiling to 4096.

In the Puddle World task, the learning rate is uniformly set to 0.01×0.999999^t . the parameter of dictionary construct is set to $\mu_1 = 0.1$, $\sigma_1 = 1$ and the parameter of kernel function

TABLE III
DICTIONARY STABILITY OF OAKTD IN VARIOUS ENVIRONMENTS.

| Environment | Dictionary Size | $\frac{\text{Convergence Steps}}{\text{Training Steps}} \times 100\%$ |
|--------------|-------------------|---|
| Mountain Car | 80.35 ± 4.32 | 0.59 ± 0.22 |
| Acrobot | 5.20 ± 2.54 | 0.23 ± 0.18 |
| Cartpole | 90.85 ± 18.23 | 0.29 ± 0.10 |
| Puddle World | 181.65 ± 7.13 | 0.36 ± 0.13 |

is set to $\sigma_2 = 0.1$. In OAKTD, we set to the slow learning rate $\alpha_t = 0.1 \times 0.99999^t$ and the fast learning rate $\beta_t = 0.01 \times 0.999999^t$. In OSKTD, we set to selective function $\mu_2 = 1.4$. In addition, in TD with Tile Coding, we set the number of tilings to 16, the size of every tiling to 512.

C. Results and Analysis

In the learning process, each algorithm runs over 50 times, each with one million steps. For online dictionary construction in our proposed OAKTD algorithm, we record the mean and std of the dictionary size after convergence, and the mean and std of the time steps (in percentage of learning steps) taken when the dictionary converges, as shown in Table III. It is easy to find that the convergence steps of the online dictionary construction are far fewer than the learning steps. It verifies the assumption that the online dictionary construction converges first.

In addition, in order to effectively evaluate the performance of different algorithms, we test the performance of the algorithm every thousand learning steps. The learning curves of several algorithms for different control tasks are shown for the first 100,000 steps in Fig. 3. In Mountain Car, from the perspective of cumulative rewards, compared with OKTD and OSKTD, OAKTD has higher mean and lower standard deviation. Compared with TD with Tile Coding, OAKTD has a faster convergence rate and approximate mean, but their final convergence results are very similar. To further reflect the behavior of OAKTD, we sample the total state space that is a set of 171×141 points evenly spaced in the position-velocity

space, as the initial state of Mountain Car. In particular, the position (velocity) interval is evenly divided into subintervals of length 0.01 (0.001). As shown in Fig. 4, TD with Tile Coding has more light streaks in the cool colors, which shows agent needs more steps in these areas. OAKTD has more smooth performance. Moreover, the number of OAKTD parameters is also far less than TD with Tile Coding. After the above analysis, OAKTD has the best performance for Mountain Car.

In the other tasks, the performance of TD with Tile Coding is relatively declined in 2-dimensional Puddle World, and 4-dimensional Acrobot and CartPole, compared to 2-dimensional Mountain Car. OKTD and OSKTD have the worst standard deviation in Acrobot and Puddle World, and don't even work in CartPole. However, OAKTD has best mean and standard deviation. The steady performance of OAKTD in the three control problems further expands the advantage of attentive function in online RL. Furthermore,

To accurately describe the attention on the kernels, based on behavior of OAKTD in Mountain Car, we sample three states $(-1, -0.07)$, $(0, 0)$, $(0.5, 0.07)$, a dictionary, and attentive parameters $w = (-0.13, -0.04)$. After standardization, visualization of attention is shown in Fig. 5. It vividly shows that attention is distributed in the kernel functions as the degree of sparsification. To further describe the distribution situation, we selected state $(0, 0)$ and visualized its attention distribution in the whole state space. As shown in Fig. 6, we can observe that attention is focused around itself and spreads outward. The experimental results show the attentive function can be well suited for sparse representation learning, and attentive kernel-based VFA can be more suitable for online RL.

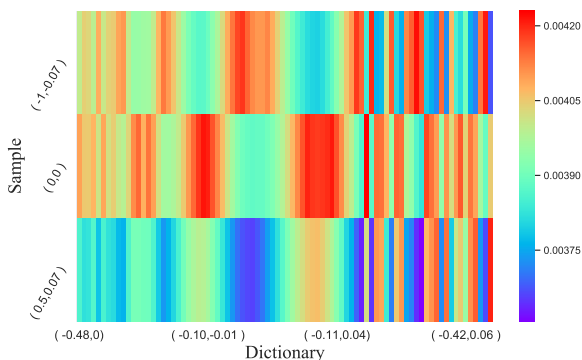


Fig. 5. Visualized in the color image is the state's attention on the kernels.

VI. CONCLUSION AND FUTURE WORK

In this paper, we construct an attentive kernel-based model and proposed a stable Online Attentive Kernel-based Temporal Difference (OAKTD) learning algorithm based on two-timescale optimization in order to simplify the model and alleviate catastrophic interference for online Reinforcement Learning (RL). Furthermore, we prove the convergence of our proposed algorithm. For the four classic control tasks

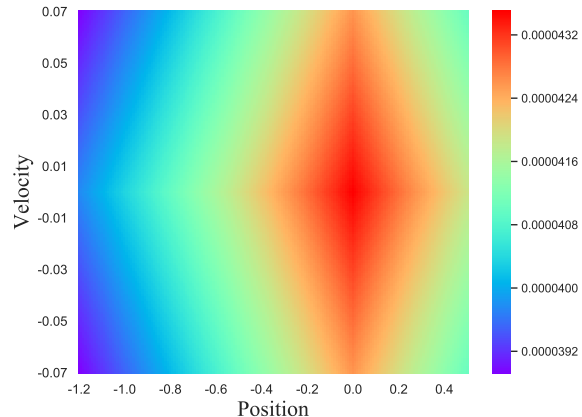


Fig. 6. Visualized in the color image is the state's attention on the whole state space.

(Mountain Car, Acrobot, CartPole and Puddle World), our experimental results verify that compared with OSKTD, OKTD and TD with Tile Coding, OAKTD performed the best.

For future study, we will focus on the following aspects: (i) to extend our OAKTD algorithm to handle continuous action RL problems, e.g., combining policy gradient or its variants [34], [35]; (ii) other ways of sparse representation that satisfy the proposed four characteristics: learnable, non-prior, non-truncated and explicit; (iii) to guarantee the stability of the algorithm, we utilize two-timescale optimization and we wish to know if other optimizations (e.g., semi-gradient method) could result in a convergence guarantee? (iv) since our proposed attentive kernel-based model is applied to the temporal difference learning algorithm, it could obviously be applied to other machine learning algorithms as well, e.g., attentive Support Vector Machine (SVM), attentive Support Vector Regression (SVR) etc.

ACKNOWLEDGEMENT

The authors would like to thank the anonymous referees and the editor for their helpful comments and suggestions.

REFERENCES

- [1] R. S. Sutton and A. G. Barto, *Reinforcement learning: An introduction*. Cambridge, MA: USA: MIT Press, 2018.
- [2] V. Liu, "Sparse representation neural networks for online reinforcement learning," Ph.D. dissertation, University of Alberta, 2019.
- [3] V. Liu, R. Kumaraswamy, L. Le *et al.*, "The utility of sparse representations for control in reinforcement learning," in *Proc. 33rd AAAI Conf. Artif. Intell.*, Honolulu, Hawaii, USA, January 2019, pp. 4384–4391.
- [4] R. S. Sutton, "Learning to predict by the methods of temporal differences," *Mach. Learn.*, vol. 3, no. 1, pp. 9–44, 1988.
- [5] Y. LeCun, Y. Bengio, and G. Hinton, "Deep learning," *Nature*, vol. 521, no. 7553, pp. 436–444, May. 2015.
- [6] R. S. Sutton, H. R. Maei, D. Precup *et al.*, "Fast gradient-descent methods for temporal-difference learning with linear function approximation," in *Proc. 26th Int. Conf. Mach. Learn.*, Montreal, Quebec, Canada, Jun. 2009, pp. 993–1000.
- [7] J. Sun, G. Wang, G. B. Giannakis *et al.*, "Finite-time analysis of decentralized temporal-difference learning with linear function approximation," in *Proc. 23rd Int. Conf. Artif. Intell. Stat.*, Palermo, Sicily, Italy, Aug. 2020, pp. 4485–4495.

- [8] D. Lee and N. He, “Target-based temporal-difference learning,” in *Proc. 36th Int. Conf. Mach. Learn.*, Long Beach, California, USA, Jun. 2019, pp. 3713–3722.
- [9] D. Ormonoit and Ś. Sen, “Kernel-based reinforcement learning,” *Mach. Learn.*, vol. 49, no. 2-3, pp. 161–178, 2002.
- [10] X. Chen, Y. Gao, and R. Wang, “Online selective kernel-based temporal difference learning,” *IEEE Trans. Neural Netw. Learn. Syst.*, vol. 24, no. 12, pp. 1944–1956, 2013.
- [11] R. S. Sutton, “Generalization in reinforcement learning: Successful examples using sparse coarse coding,” in *Proc. Adv. Neural Inf. Process. Syst. 9*, Denver, CO, USA, Dec. 1996.
- [12] K. Krawiec and M. G. Szubert, “Learning n-tuple networks for othello by coevolutionary gradient search,” in *Proc. 13th Ann. Conf. Genet. Evolut. Comput.*, Dublin, Ireland, Jul. 2011, pp. 355–362.
- [13] V. Nair and G. E. Hinton, “Rectified linear units improve restricted boltzmann machines,” in *Proc. 27th Int. Conf. Mach. Learn.*, Haifa, Israel, Jun. 2010, pp. 807–814.
- [14] N. Srivastava, G. Hinton, A. Krizhevsky *et al.*, “Dropout: a simple way to prevent neural networks from overfitting,” *J. Mach. Learn. Res.*, vol. 15, no. 1, pp. 1929–1958, 2014.
- [15] A. Makhzani and B. Frey, “K-sparse autoencoders,” in *Proc. 2nd Int. Conf. Learn. Repr.*, Banff, AB, Canada, Apr. 2014.
- [16] A. Makhzani and B. J. Frey, “Winner-take-all autoencoders,” in *Proc. Adv. Neural Inf. Process. Syst. 28*, Montreal, Quebec, Canada, December 2015, pp. 2791–2799.
- [17] M. Y. Park and T. Hastie, “L1-regularization path algorithm for generalized linear models,” *J. Royal Stat. Soc.*, vol. 69, no. 4, pp. 659–677, 2007.
- [18] F. Girosi, M. Jones, and T. Poggio, “Regularization theory and neural networks architectures,” *Neural Comput.*, vol. 7, no. 2, pp. 219–269, 1995.
- [19] K. Xu, J. Ba, R. Kiros *et al.*, “Show, attend and tell: Neural image caption generation with visual attention,” in *Proc. 32nd Int. Conf. Mach. Learn.*, Lille, France, Jul. 2015, pp. 2048–2057.
- [20] V. Mnih, N. Heess, A. Graves *et al.*, “Recurrent models of visual attention,” in *Proc. Adv. Neural Inf. Process. Syst. 27*, Montreal, Quebec, Canada, Dec. 2014, pp. 2204–2212.
- [21] D. Bahdanau, K. Cho, and Y. Bengio, “Neural machine translation by jointly learning to align and translate,” in *Proc. 3rd Int. Conf. Learn. Repr.*, San Diego, CA, USA, May. 2014.
- [22] W. Chung, S. Nath, A. Joseph *et al.*, “Two-timescale networks for nonlinear value function approximation,” in *Proc. 7th Int. Conf. Learn. Repr.*, New Orleans, LA, USA, May. 2019.
- [23] B. Schölkopf, R. Herbrich, and A. J. Smola, “A generalized representer theorem,” in *Proc. Int. Conf. Comput. Learn. Theory*, Berlin, Heidelberg, 2001, pp. 416–426.
- [24] W. Liu, I. Park, and J. C. Principe, “An information theoretic approach of designing sparse kernel adaptive filters,” *IEEE Trans. Neural Netw.*, vol. 20, no. 12, pp. 1950–1961, 2009.
- [25] L. Baird, “Residual algorithms: Reinforcement learning with function approximation,” in *Proc. 12th Int. Conf. Mach. Learn.*, Tahoe City, California, USA, Jul. 1995, pp. 30–37.
- [26] H. R. Maei, C. Szepesvári, S. Bhatnagar *et al.*, “Convergent temporal-difference learning with arbitrary smooth function approximation,” in *Proc. Adv. Neural Inf. Process. Syst. 22*, Vancouver, British Columbia, Canada, Dec. 2009, pp. 1204–1212.
- [27] Y. Engel, S. Mannor, and R. Meir, “The kernel recursive least-squares algorithm,” *IEEE Trans. Neural Netw. Learn. Syst.*, vol. 52, no. 8, pp. 2275–2285, 2004.
- [28] X. Xu, D. Hu, and X. Lu, “Kernel-based least squares policy iteration for reinforcement learning,” *IEEE Trans. Neural Netw. Learn. Syst.*, vol. 18, no. 4, pp. 973–992, 2007.
- [29] V. S. Borkar, “Stochastic approximation with two time scales,” *Syst. & Cont. Lett.*, vol. 29, no. 5, pp. 291–294, 1997.
- [30] G. Teschl, *Ordinary Differential Equations and Dynamical Systems*. American Mathematical Society, 2012.
- [31] H. J. Kushner and D. S. Clark, *Stochastic approximation methods for constrained and unconstrained systems*. Springer Science & Business Media, 2012.
- [32] V. S. Borkar, *Stochastic approximation: a dynamical systems viewpoint*. Springer, 2009.
- [33] D. A. Levin and Y. Peres, *Markov chains and mixing times*. American Mathematical Society, 2017.
- [34] T. P. Lillicrap, J. J. Hunt, A. Pritzel *et al.*, “Continuous control with deep reinforcement learning,” in *Proc. 4th Int. Conf. Learn. Repr.*, San Juan, Puerto Rico, May. 2016.
- [35] V. Mnih, A. P. Badia, M. Mirza *et al.*, “Asynchronous methods for deep reinforcement learning,” in *Proc. 33rd Int. Conf. Mach. Learn.*, New York City, NY, USA, Jun. 2016, pp. 1928–1937.